Salinet, J.; Schlindwein, FS.; Stafford, P.; Almeida, TP.; Li, X.; Vanheusden, F.; Guillem Sánchez, MS.... (2017). Propagation of meandering rotors surrounded by areas of high dominant frequency in persistent atrial fibrillation. Heart Rhythm. 14(9):1269-1278. https://doi.org/10.1016/j.hrthm.2017.04.031

# PROPAGATION OF MEANDERING ROTORS SURROUNDED BY HIGH DOMINANT FREQUENCY AREAS IN PERSISTENT ATRIAL FIBRILLATION

João Salinet[#†], PhD, Fernando S. Schlindwein[‡~], PhD, DSc, Peter Stafford[§], MB BS, MD, FRCP, Tiago P. Almeida[#‡], PhD, Xin Li[‡], PhD, Frederique J. Vanheusden[‡], PhD, María S. Guillem[#*], PhD, G. André Ng[‡~§*], MBChB, PhD, FRCP(Glasg), FRCP, FESC. [#]Engineering, Modelling and Applied Social Sciences Centre, Federal ABC University, Brazil; [†]Bioengineering Division of the Heart Institute (Incor), University of São Paulo, Brazil; [‡]Departments of Engineering and Cardiovascular Sciences, University of Leicester, UK; ~NIHR Leicester Cardiovascular Biomedical Research Unit; [§]University Hospitals of Leicester NHS Trust, UK; [#]ITACA, Universitat Politècnica de València, Valencia, Spain.

* Dr. María Guillem and Professor G. André Ng have contributed equally on the manuscript co-sharing the senior authorship.

**Address for correspondence:**
Dr. João Salinet
Engineering, Modelling and Applied Social Sciences Centre, Federal ABC University
São Bernardo do Campo, São Paulo, Brazil, 09606-070
Tel: +55 11 2320 6342
Email: joao.salinet@ufabc.edu.br

**Short title:** Co-localized Drifting Rotors in Atrial Fibrillation

**Total of words:** 5,000

**Conflict of Interest**

Prof. Ng received research fellowships from St. Jude Medical and speaker fees and honoraria from Biosense Webster. All other authors have no relationships to disclose.

**Funding Sources**

This work was supported by the Leicester NIHR Cardiovascular Biomedical Research Unit, UK. Dr. Salinet was supported by CNPq 200598/2009-0 and FAPESP #2014/26066-0. Dr. Almeida was funded by CNPq 200598/2009-0.

**Abstract**

**Background:** identification of arrhythmogenic regions remains a challenge in persistent atrial fibrillation (persAF). Frequency and phase analysis allows identification of potential ablation targets.

**Objective:** This study aims to investigate the spatiotemporal association between dominant frequency (DF) and re-entrant phase activation areas.

**Methods:** Eight persAF patients undergoing first-time catheter ablation procedure were enrolled. A non-contact array catheter was deployed into the left atrium (LA) and 2048 AF electrograms (AEG) were acquired for 15 seconds following ventricular far-field cancellation. DF and phase singularity (PS) points were identified from the AEGs and tracked over consecutive frames. The spatiotemporal correlation of high DF areas and PS points was investigated and the organization index of high DF areas was compared with their periphery.

**Results:** The phase maps presented multiple simultaneous PS points that drift over the LA, with preferential locations. Regions displaying higher PS concentration showed a degree of co-localization with DF sites, with PS and DF regions being neighbors in 61.8% and with PS and DF regions overlapping 36.8% of the time windows. Sites with highest DF showed a greater degree of organization at their core (CG) compared to their periphery. After ablation, the PS incidence reduced over the entire LA (36.2±23.2%, $p<0.05$), but especially at the pulmonary veins (PVs) (78.6±22.2%, $p<0.05$).

**Conclusions**: Multiple PS points drifting over the LA were identified with their clusters correlating spatially with the DF regions. After PV isolation, the PS's complexity was reduced, which supports the notion that PS sites represent areas of relevance to the atrial substrate.

**Key Words:** atrial fibrillation, phase singularity, dominant frequency, non-contact mapping, ablation.

## Introduction

The theory of atrial fibrillation (AF) in humans suggests the existence of multiple mechanisms involved in the AF initiation and perpetuation, including re-entrant circuits, rapidly firing foci and high frequency sites.[1-3] These mechanisms are believed to be more pronounced in patients whose AF persists for long-term periods (persAF) or in which noticeable electrical and structural atrial substrate remodeling are observed.[4] However, the characterization of arrhythmogenic atrial regions for successful ablation in the presence of concurrent fibrillatory mechanisms remains a challenge, usually requiring multiple procedures.[4]

Ablation strategy guided by dominant frequency (DF) resulted in interatrial DF gradient reduction, prolonging patients' sinus rhythm maintenance. [5] High-density DF mapping of persAF allowed recognition of dynamic spatiotemporal patterns,[6] suggesting that ablation therapy is unlikely to be successful by observing a single time frame. Investigators identified AF re-entry sources using phase analysis techniques in invasive[7] and non-invasive[8] electrophysiology (EP) systems. They also showed that targeting these sources appears to improve treatment success. The relationship between DF and phase has been assessed in intracardiac contact recordings.[9, 10] Those studies have shown that highest DF boundary areas were circumscribed by rotors, suggesting the occurrence of wavebreaks close to these boundary areas. However, the relationship between frequency and phase analyses on non-contact mapping (NCM) has not been fully understood and the spatiotemporal associations between DF and phase singularity (PS) re-entrant activity is of interest for the study of the mechanisms involved in the genesis and maintenance of persAF.

The study aims were (1) to investigate the feasibility of high-density phase mapping of the left atrium (LA) substrate to identify arrhythmogenic sites and circuits during persAF and, (2) to study the association between PS and high DF (HDF) activity in the LA substrate during persAF.

## Methods

### *Electrophysiological Study*

Eight patients undergoing first time persAF catheter ablation were recruited. All patients were in AF at the start of the NCM procedure. Approval was obtained from the local ethics committee and informed consent was obtained before the study was conducted. Antiarrhythmic drugs, apart from amiodarone, were stopped for at least five half-lives before the procedure. The multi-electrode array (MEA) catheter (EnSite 3000, St Jude Medical, USA) was deployed via trans-septal access, into the LA. The MEA is an intracardiac catheter with a central lumen and pigtail tip introduced with guide wire into the cardiac chamber with the working component being a wire mesh with 64 laser-etched electrodes mounted on a collapsible balloon at the distal end of the catheter. NCM employs inverse solution mathematics to produce virtual unipolar electrograms from far-field electrograms collected from the electrodes. Details of the mapping procedure have been described elsewhere[6] and in the supplementary material.

### *Signal Processing*

AEGs were sampled at 1200 Hz and 15-seconds long segments of non-induced persAF data were exported for off-line analysis. The AEGs were band-pass filtered between 3 Hz

and 30 Hz with a tenth-order zero-phase delayed Butterworth filter. Ventricular far-field influence cancellation was performed using a customized and adaptive QRS-T segmentation algorithm followed by a coherent subtraction strategy (supplementary material).[11]

*Phase Analysis*

The phase representation of each AEG was obtained and NCM phase maps were created to obtain sequential maps with automatic PS identifications. Firstly, a Hilbert transform is applied to the AEG to produce an analytic signal, then the phase was found as the inverse tangent of the ratio of imaginary and real part of the analytic signal (Figure 1A).[10] Thus, for each sample, the calculated phase was limited between $-\pi$ and $+\pi$ and the color scale of an activation is illustrated in Figure 1A. Once phase analysis was applied to all 2048 AEGs, sequential 2D and 3D phase maps were developed. A 2D phase frame (and its respective 3D plot) are presented in Figure 1B, highlighting a PS point and four distinct progressive phase regions representing the $[-\pi\ +\pi]$ cycle. The spatial phase distributions were analyzed to locate PS points. PSs were automatically identified by determining at locations around which the phase progresses through a complete cycle from $-\pi$ to $+\pi$.[10, 12] Only PS points lasting over consecutive frames for at least 100 ms[9] were considered. The respective AEGs and their phase delays are presented in Figure 1C. Figure 1D shows the spatiotemporal wavefront propagation of a complete phase progress rotation, observed over four frames. The arrows show the phase propagation direction and the yellow circle shows the PS position.

*Frequency Analysis*

Spectral analysis consisted of identifying the DF – defined as the frequency with the highest power within 4 Hz to 10 Hz – to produce sequential 2D and 3D DF density maps of the LA.[6] Fast Fourier Transform (FFT) with a Hamming window was applied on the 2048 AEGs on sequential segments of 4 s windows with 50% overlap (shifting forward by 2 s) to produce consecutive 3D DF maps. The spectral resolution was 0.25 Hz and zero padding was applied to produce frequency steps of 0.05 Hz.

An organization index (OI) was calculated by dividing the area under the DF and its harmonics by the total area of the spectrum between 4 Hz and 20 Hz. For each sequentially obtained DF map, the highest DF areas (HDFA) were defined as the atrial regions within a 0.25 Hz drop from the highest DF.[6] The center of gravity (CG) of the HDFA was then found. OI was computed as the mean OI in the HDFA-CG (CG point plus its 8 closest neighbors) ($OI_{CG}$) and the mean OI at periphery ($OI_{Per}$) was computed as the average of the OI at all sites in the DF area boundary.

*Phase and Frequency Spatiotemporal Analysis*

The behavior of the DF maps was investigated with both highest (HDF) and lowest DF (LDF) areas identified automatically. These areas contain the values within 0.25 Hz of the HDF and LDF respectively. This would present an area that reflects the average local activity, minimizing the effect of isolated DF sites.

The spatiotemporal correlation between DF and PS regions was studied by observing the geometric relationship between LA areas containing high frequency activation and high

incidence of singularities. If higher PS occurrence was within the boundaries of the HDF areas and/or located nearby (up to 5 adjacent nodes) then DF and PS regions were considered to being co-localized. Phase and frequency analysis[6, 13] were performed using in-house custom written software.

### *Statistical analysis*

All continuous variables are expressed as mean ± standard deviation. Shapiro-Wilk normality test was performed. Non-parametric data was log-transformed. A multivariate analysis (MANOVA) was performed to determine differences between the groups and Tukey post hoc tests were conducted. P-values of less than 0.05 were considered statistically significant.

## Results

Patients' characteristics are summarized on Table 1. Post-processing of signals and phase singularities identification of each of these 15 s windows required 18.91±0.99 seconds in a desktop PC Intel® Xeon® Processor E5-1630v4 @ 3.70 GHz, 32 GB RAM, 3TB 7200 rpm hard drive with a Windows 10 Pro 64bit.

### Spatiotemporal behavior of phase singularities

The detected PSs were systematically tracked over consecutive time frames. PSs typically appeared in pairs and were not spatially anchored at particular sites. Instead they drifted over the LA area (Figure 2 and Movie S1). Overall, PSs were observed during 16.90±5.89% of the time and lasted for 188.25±62.59 ms. The longest PS observed lasted for 416.70 ms.

Despite the observed PS drift, the PS histograms demonstrated preferential areas where these PSs appear more often. A sample case is presented in Figure 3A for three different patients. Regions close to the pulmonary veins (PVs) and roof presented a higher concentration of PS points when compared with the remaining LA areas. Figure 3B is a graphic representation of the highest incidence of PSs considering all the patients. Areas close to the PV, followed by the roof, had nearly 72% of the identified PSs (445 out of 617). Floor and posterior wall (PW) regions presented moderated incidences of PSs in 15 seconds long segments of persAF recordings.

**Phase singularities after substrate modification**

PV ablation had a significant impact on PS occurrence (Figure 4). At baseline (Figure 4A) the roof, PW and anterior wall presented a higher incidence of PSs than other LA locations. The impact of the ablation can be observed in Figure 4B. The total number of occurrences significantly reduced, and the pattern of the histogram was also modified after PVI. In the population under study, the PS incidence was reduced from 2854.4±736.9 to 1770.2±635.7 ($p<0.05$), an overall reduction of 36.2±23.2%. Subdividing it into two groups, PV areas and non-PV areas, the percentage of reduction was respectively 78.6±22.2% ($p<0.05$) and 36.8±24.8% ($p=0.05$). A detailed analysis is presented in Figure 4C.

**Physiological meaning of PSs in persAF and its relation with the anatomical substrate**

The PS occurrence reduction on the PVs was more prominent (90.8±59.8 to 23.8±31.6, 78.6±22.2% $p<0.05$). This decrease in PS incidence was observed in all PVs (Figure 4C).

The singularities were mostly located close to the right PV, with the RSPV being most prominent. The LIPV presented a higher incidence of PSs than the LSPV. After PVI, no PSs were found at the LSPV.

**Relationship between highest DF sites and PSs**

To investigate the detected PS sites driving nature, we studied the spatial correlation of HDF sites with sites with higher PS incidence. In total, 156 maps (78 pairs of DF and phase histogram maps) were studied with 96 at baseline and 60 post PVI. HDF regions and highest PS occurrence did not always match. A spatial correspondence was found between both areas in 87.2% of the time segments under study. Spatial correspondence means that a DF site is close to or overlaps the region with the higher PS incidence for the same time segment (Figure 5). In Figure 5A, the PSs higher occurrence is found close to the HDF regions boundary. This pattern was observed in 61.8% of the time segments. In Figure 5B, there is some overlap between HDF and highest PS occurrence regions. Overall, a partial overlap between both regions was observed in 36.8% of the time segments.

Highest DF sites typically showed a higher OI at their core (i.e., the CG) when compared to the periphery and increased again organization at sites distant from the highest DF (Figure 6). The MANOVA showed significant interactions between groups ($F=6.1$, $p=0.009$). In the population, OI at the core was $0.422\pm0.101$ vs. periphery $0.386\pm0.126$ ($p=0.02$). Similarly, OI at their core still tended to be higher as compared to their periphery after PVI ($0.372\pm0.026$ vs. $0.332\pm0.036$, $p=0.22$). After PVI, ablation significantly decreased the OI at the core and at the periphery when compared with

baseline (OI core: 0.372±0.026 vs. 0.422±0.101, p<0.0001; OI periphery: 0.332±0.036 vs. 0.386±0.126, p<0.0001).

## Discussion

In this study, we showed that high-density phase mapping could be performed from simultaneous NCM AEGs obtained from persAF patients to allow investigation of potential arrhythmogenic sites and circuits. In addition, studying the wavefront spatiotemporal propagation enables investigators to identify multiple paired PS points that are not anchored at specific regions, drifting over different areas of the LA, with more prominent clustering in regions close to PV and roof and related with the atrial substrate.

### Phase mapping and dynamics of the singularities

PSs during cardiac fibrillation have been demonstrated to be a pivot of functional re-entrant circuits[10] and are important for mapping fibrillatory patterns[12] in both animal and human studies.[7, 13-14] Narayan *et al.* have shown that ablation of rotor sites in persAF patients results in longer AF-free periods than a PVI-only strategy. [15] This is consistent with the experimental findings of rotors sustaining AF in animal models that have been reported over the last few years.[12, 16] Recently, Hansen *et al.*, have reported structural micro-reentries as the underlying mechanism sustaining human AF[17] and have shown a good correspondence between optical mapping and FIRM mapping data.[18] Our results, with preferential locations for PSs in persAF patients, are consistent with these findings of rotors that may anchor at specific sites with partially disconnected atrial bundles or electrically partially isolated regions due to extensive fibrosis. However, in our mapping data, PSs are less stable and not anchored to fixed locations.

Recent studies have failed to reproduce the favorable outcomes of FIRM-guided ablation.[19-20] Differences in patient recruitment may contribute to these diverging results. However, arguments regarding the validity of the methodology and the underlying AF mechanisms are justified. It may be argued that phase mapping by applying Hilbert's transform may contribute to artifactual PSs that are not related to the actual tissue electrical activity. [21] However, we have found that most of the detected PSs are related with the electrical or anatomical substrate since ablation reduced their occurrence significantly.

Additionally, we have shown that PSs are more likely to be located at the PVs and roof followed by the PW and floor (Figure 3). These findings are in agreement with recent human studies where rotors were not stationary but drifted mostly around the LA (from PVs to LA).[8] The PVs and PW have also been previously indicated to play an important role in AF maintenance by high-frequency re-entrant sources.[2, 22-23]

**PSs role in the maintenance of AF**

Animal models of acetylcholine-induced AF have consistently shown that driving rotors activate at the fastest rate in the atria while fractionation of the wavefront results in fibrillatory conduction at a slower and less organized rate.[22] In line, spectral analysis has been used as an auxiliary investigative tool in an attempt to understanding certain physiological AF mechanisms and patterns.[2, 22, 24] Spatiotemporal stable atrial sources represented by HDF were seen in human AF in both invasive and non-invasive studies.[5, 25-26] Interestingly, ablation of these areas has been shown to be an effective therapy to restore sinus rhythm.[5, 26]

From our observations, the PS rotors do not exactly match the highest DF locations. However, we found some degree of correlation between PS and HDF regions, since only few DF maps (13%) had no cumulative PSs inside the HDF areas and LA regions showing high concentration of singularities are frequently neighboring or even invading areas harboring HDFs (Figure 5).

We can attribute both the instability of PSs and their correspondence lack with the HDF sites mainly to: (1) a more complex behavior interplay of PS and HDF areas than a simple spatial matching; (2) lack of high-frequency driving rotors in our analyzed data and/or (3) methodological limitations. It has been well documented that persAF are less likely to present DF gradients[27] and, therefore it is not unlikely that driving rotors in persAF may not activate significantly faster than other atrial regions. In addition, AF drivers may be located outside the LA in persAF and thus, some of the driving sites may reside outside our mapped region. The detected PSs may not have a driving role in our population and they could be just bystanders or sites at which the electrical activation transiently turns or breaks. Further investigations on ablating these sites would be necessary to provide insight on the detected PSs driving role. Although we could not confirm the driving role of highest DF sites or the areas with more cumulative PSs we did observe an increased organization in the HDF area and disorganization at its periphery, consistent with a hierarchical activation from the highest DF site and wave fractionation at the boundaries.[28] The PS incidence reduction due to ablation was also related with more organized AEGs in the HDF core rather than periphery. This may indicate that PVI promoted both spatial and temporal organization of the AEGs at these HDF sites.

The lack of spatial consistency in our detected PSs may be related to the influence of far-field artifacts that may not accurately represent endocardial potentials. NCM system has been validated in the clinical setting[29-30] in the time and frequency domains[31-32] providing an important tool that can contribute to the understanding of cardiac arrhythmias. Further studies have shown that AF non-contact recordings suffer from an artifactual meandering of the rotor tip, simplification of activation patterns and appearance of dual (or 'mirror') PSs.[13] These observations are consistent with the current study, since PSs are unstable but non-random because they cluster at preferential locations. Our reported potential maps are also simpler than previously reported epicardial maps[33] but similar to surface[13] or inverse-computed maps.[34-35] Finally, our reported PSs appear in pairs, which is most likely reflecting a single rotation seen from two contralateral points of view. However, in spite of all the noted limitations of non-contact recordings, they may retain some key features of the underlying propagation pattern such as the preferential location of PS sites[13] and, therefore, may be useful for ablation guidance.[15, 18]

**Limitations**

This study involved a small number of patients, as our main objective was to study phase mapping using high-density NCM in persAF and investigate the behavior of PS and DF. AEG analysis was restricted to the LA, hence any potential contribution from the right atrium was not studied. Three patients could not have their post-ablation data exported. Nevertheless, the results presented were consistent in all patients.

## Conclusions

Non-contact phase mapping of persAF appears to be a reliable technique to investigate potential arrhythmic re-entrant activity. Multiple dynamic paired PS points were identified and their clusters correlated with the DF regions, although may be influenced by far-field artifacts, seem to be associated with the underlying atrial substrate. Whilst we could not determine the driving role of these re-entrant sites, combined real-time DF and PS mapping may contribute to identify important arrhythmogenic atrial regions that might be useful for designing an effective ablation strategy in persAF treatment.

## References:


**1.** Haissaguerre M, Jais P, Shah DC, Garrigue S, Le Mouroux A, Le Métayer P, Clémenty J. Spontaneous initiation of atrial fibrillation by ectopic beats originating in the pulmonary veins. N Engl J Med 1998;339:659-666.

**2.** Jalife J, Berenfeld O, Mansour M. Mother rotors and fibrillatory conduction: a mechanism of atrial fibrillation. Cardiovasc R 2002;54:204-216.

**3.** Moe GK, Rheinboldt WC, Abildskov JA. A Computer Model of Atrial Fibrillation. Am Heart J 1964;67:200-220.

**4.** Brooks AG, Stiles MK, Laborderie J, Lau DH, Kuklik P, Shipp NJ, Hsu LF, Sanders P. Outcomes of long-standing persistent atrial fibrillation ablation: a systematic review. Heart Rhythm 2010;7:835-846.

**5.** Atienza F, Almendral J, Jalife J, Zlochiver S, Ploutz-Snyder R, Torrecilla EG, Arenal A, Kalifa J, Fernández-Avilés F, Berenfeld O. Real-time dominant frequency mapping and ablation of dominant frequency sites in atrial fibrillation with left-to-right frequency gradients predicts long-term maintenance of sinus rhythm. Heart Rhythm 2009;6:33-40.

**6.** Salinet JL, Tuan JH, Sandilands AJ, Stafford PJ, Schlindwein FS, Ng GA. Distinctive patterns of dominant frequency trajectory behavior in drug-refractory persistent atrial fibrillation: preliminary characterization of spatiotemporal instability. J Cardiovasc Electrophysiol 2014;25:371-379.

**7.** Narayan SM, Patel J, Mulpuru S, Krummen DE. Focal impulse and rotor modulation ablation of sustaining rotors abruptly terminates persistent atrial fibrillation to sinus rhythm with elimination on follow-up: a video case study. Heart Rhythm 2012;9:1436-1439.

**8.** Haissaguerre M, Hocini M, Denis A et. al. Driver domains in persistent atrial fibrillation. Circulation 2014;130:530-538.

**9.** Samie FH, Berenfeld O, Anumonwo J, Mironov SF, Udassi S, Beaumont J, Taffet S, Pertsov AM, Jalife J. Rectification of the background potassium current: a determinant of rotor dynamics in ventricular fibrillation. Circ Res 2001;89:1216-1223.

**10.** Umapathy K, Nair K, Masse S, Krishnan S, Rogers J, Nash MP, Nanthakumar K. Phase mapping of cardiac fibrillation. Circ Arrhythm Electrophysiol 2010;3:105-114.

**11.** Salinet JL, Madeiro JPV, Cortez PC, Stafford PJ, Ng GA, Schlindwein FS. Analysis of QRS-T subtraction in unipolar atrial fibrillation electrograms. Med Biol Eng Comput 2013;51:1381-1391.

**12.** Pandit SV, Jalife J. Rotors and the dynamics of cardiac fibrillation. Circ Res 2013;112:849-862.

**13.** Rodrigo M, Guillem M, Climent AM, Pedrón-Torrecilla J, Liberos A, Millet J, Fernández-Avilés F, Atienza F, Berenfeld O. Body Surface Localization of Left and Right Atrial High Frequency Rotors in Atrial Fibrillation Patients: a clinical-computational study. Heart Rhythm 2014;11:1584-1591.

**14.** Haissaguerre M, Hocini M, Shah AJ, Derval N, Sacher F, Jais P, Dubois R. Noninvasive Panoramic Mapping of Human Atrial Fibrillation Mechanisms: a feasibility report. J Cardiovasc Electrophysiol 2013;24:711-717.

**15.** Narayan SM, Krummen DE, Shivkumar K, Clopton P, Rappel WJ, Miller JM. Treatment of atrial fibrillation by the ablation of localized sources: CONFIRM (Conventional Ablation for Atrial Fibrillation With or Without Focal Impulse and Rotor Modulation) trial. J Am Coll Cardiol. 2012;60:628-636.

**16.** Berenfeld O, Jalife J. Mechanism of atrial fibrillation: rotors, ionic determinants, and excitation frequency. Cardiol Clin 2014;32:495-506.

**17.** Hansen BJ, Zhao J, Csepe TA et. al. Atrial fibrillation driven by micro-anatomic intramural re-entry revealed by simultaneous sub-epicardial and sub-endocardial optical mapping in explanted human hearts. Eur Heart J 2015: 36:2390-401.

**18.** Hansen BJ, Briggs C, Moore BT, Csepe TA, Li N, Zhao J, Garikipati NV, Janssen PM, Mohler PJ, Hummel JD, Fedorov VV. Human Atrial Fibrillation Drivers Seen Simultaneously by Focal Impulse and Rotor Mapping and High-resolution Optical Mapping. Circulation 2015;132:A18402.

**19.** Gianni C, Mohanty S, Di Biase L et al. Acute and early outcomes of focal impulse and rotor modulation (FIRM)-guided rotors-only ablation in patients with nonparoxysmal atrial fibrillation. Heart Rhythm 2016;13:830-835.

**20.** Buch E, Share M, Tung R et al. Long-term clinical outcomes of focal impulse and rotor modulation for treatment of atrial fibrillation: A multicenter experience. Heart Rhythm 2016;13:636-641.

**21.** Kuklik P, Zeemering S, Maesen B, Maessen J, Crijns HJ, Verheule S, Ganesan AN, Schotten U. Reconstruction of instantaneous phase of unipolar atrial contact electrogram using a concept of sinusoidal recomposition and Hilbert transform. IEEE Trans Biomed Eng. 2015;62:296-302.

**22.** Mansour M, Mandapati R, Berenfeld O, Chen J, Samie FH, Jalife J. Left-to-right gradient of atrial frequencies during acute atrial fibrillation in the isolated sheep heart. Circulation 2001;103:2631-2636.

**23.** Sahadevan J, Ryu K, Peltz L, Khrestian CM, Stewart RW, Markowitz AH, Waldo AL. Epicardial mapping of chronic atrial fibrillation in patients: preliminary observations. Circulation 2004;110:3293-3299.

**24.** Habel N, Znojkiewicz P, Thompson N et al. The temporal variability of dominant frequency and complex fractionated atrial electrograms constrains the validity of sequential mapping in human atrial fibrillation. Heart Rhythm 2010;7:586-593.

**25.** Guillem MS, Climent AM, Millet J, Arenal Á, Fernández-Avilés F, Jalife J, Atienza F, Berenfeld O. Noninvasive localization of maximal frequency sites of atrial fibrillation by body surface potential mapping. Circ Arrhythm Electrophysiol 2013;6:294-301.

**26.** Sanders P, Berenfeld O, Hocini M et al. Spectral analysis identifies sites of high-frequency activity maintaining atrial fibrillation in humans. Circulation 2005;112:789-797.

**27.** Lazar S, Dixit S, Marchlinski FE, Callans DJ, Gerstenfeld EP. Presence of left-to-right atrial frequency gradient in paroxysmal but not persistent atrial fibrillation in humans. Circulation 2004;110:3181-3186.

**28.** Kalifa J, Tanaka K, Zaitsev AV et al. Mechanisms of wave fractionation at boundaries of high-frequency excitation in the posterior left atrium of the isolated sheep heart during atrial fibrillation. Circulation 2006;113:626-633.

**29.** Schilling RJ, Peters NS, Davies W. Simultaneous endocardial mapping in the human left ventricle using a noncontact catheter - comparison of contact and reconstructed electrograms during sinus rhythm. Circulation 1998;98:887-898.

**30.** Gornick CC, Adler SW, Pederson B, Hauck J, Budd J, Schweitzer J. Validation of a new noncontact catheter system for electroanatomic mapping of left ventricular endocardium. Circulation 1999;99:829-835.

**31.** Lin YJ, Higa S, Kao T, Tso HW, Tai CT, Chang SL, Lo LW, Wongcharoen W, Chen SA. Validation of the frequency spectra obtained from the noncontact unipolar electrograms during atrial fibrillation. J Cardiovasc Electrophysiol 2007;18:1147-1153.

**32.** Gojraty S, Lavi N, Valles E, Kim SJ, Michele J, Gerstenfeld EP. Dominant frequency mapping of atrial fibrillation: comparison of contact and noncontact approaches. J Cardiovasc Electrophysiol 2009;20:997-1004.

**33.** Allessie MA, Bonke FIM, Schopman FJG. Circus movement in rabbit atrial muscle as a mechanism of tachycardia. III The "leading circle" concept: a new model of circus movement in cardiac tissue without the involvement of an anatomical obstacle. Circ Res 1977;41:9-18.

**34.** Haissaguerre M, Hocini M, Denis A et. al. Driver domains in persistent atrial fibrillation. Circulation. 2014;130:530-538.

**35.** Pedrón-Torrecilla J, Rodrigo M, Climent AM, Liberos A, Pérez-David E, Bermejo J, Arenal Á, Millet J, Fernández-Avilés F, Berenfeld O, Atienza F, Guillem MS. Noninvasive Estimation of Epicardial Dominant High-Frequency Regions During Atrial Fibrillation. J Cardiovasc. Electrophysiol. 2016;27:435-442.

# Table 1

Patients' characteristics

| | n=8 |
|---|---|
| **Male, n** | 8 |
| **Age, y** | 47±10 |
| **AF duration, mo** | 34±25 |
| **Hypertension, n** | 2 |
| **LV function, n** | |
| **EF≥55%** | 5 |
| **EF 45-54%** | 2 |
| **EF 36-44%** | - |
| **EF≤35%** | 1 |
| **LA Size, mm** | 48±6 |
| **On amiodarone, n** | 3 |

# Figure 1

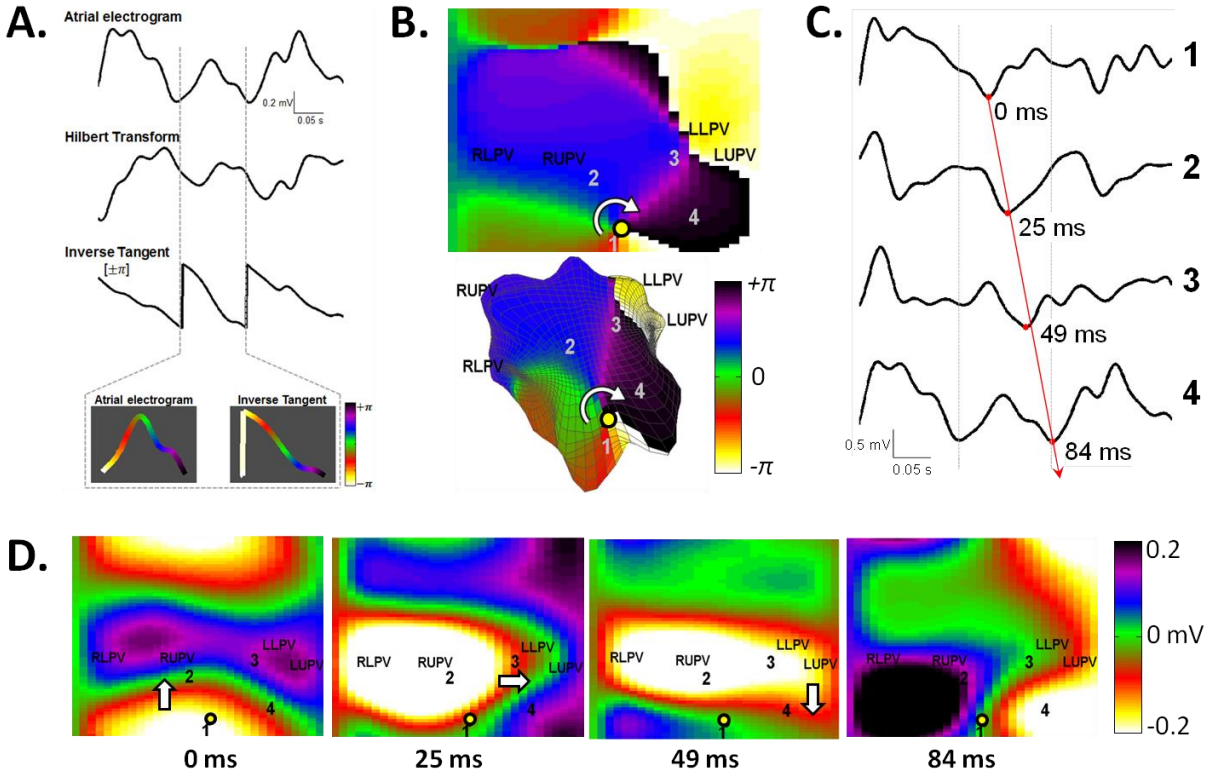


Figure 1 - The methodological procedure used to obtain phase mapping and PS in simultaneous unipolar reconstructed non-contact AEGs undergoing persAF. In (A) an illustrative example of how the surrogate phase signal is obtained from the AEG is presented. The phase of the AEG is derived from the inverse tangent of the Hilbert transform of the AEG. (B) Sample 2D phase map (and its 3D representation) for a given time instant with superimposed PS points (yellow circles). (C) Time series of selected electrograms and (D) the spatiotemporal wavefront propagation at selected time frames evidence one rotation activity with the PS point at the center.

# Figure 2

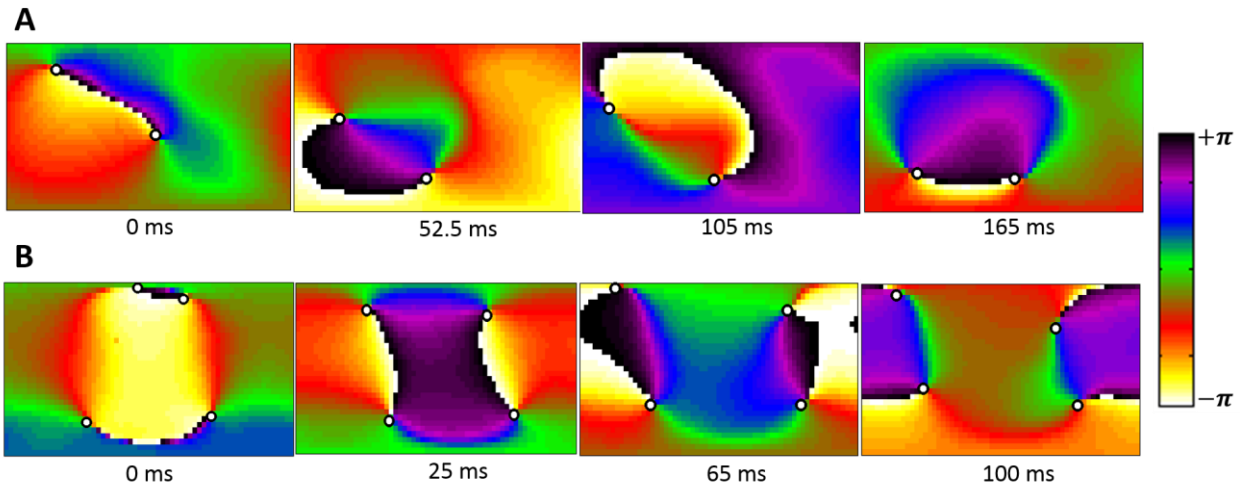


Figure 2 - A sequence of two distinct episodes of phase mapping on persAF in 2D highlighting the propagation of the paired detected PSs drifting across the LA at sequential short time steps. (A) A pair of PSs appeared near the roof (left-hand side) and moved through the LA area in a short time segment (165 ms); (B) another example of PSs propagation, with two paired PSs highlighting the presence of multiple PSs propagating simultaneous on the LA of some persAF.

# Figure 3

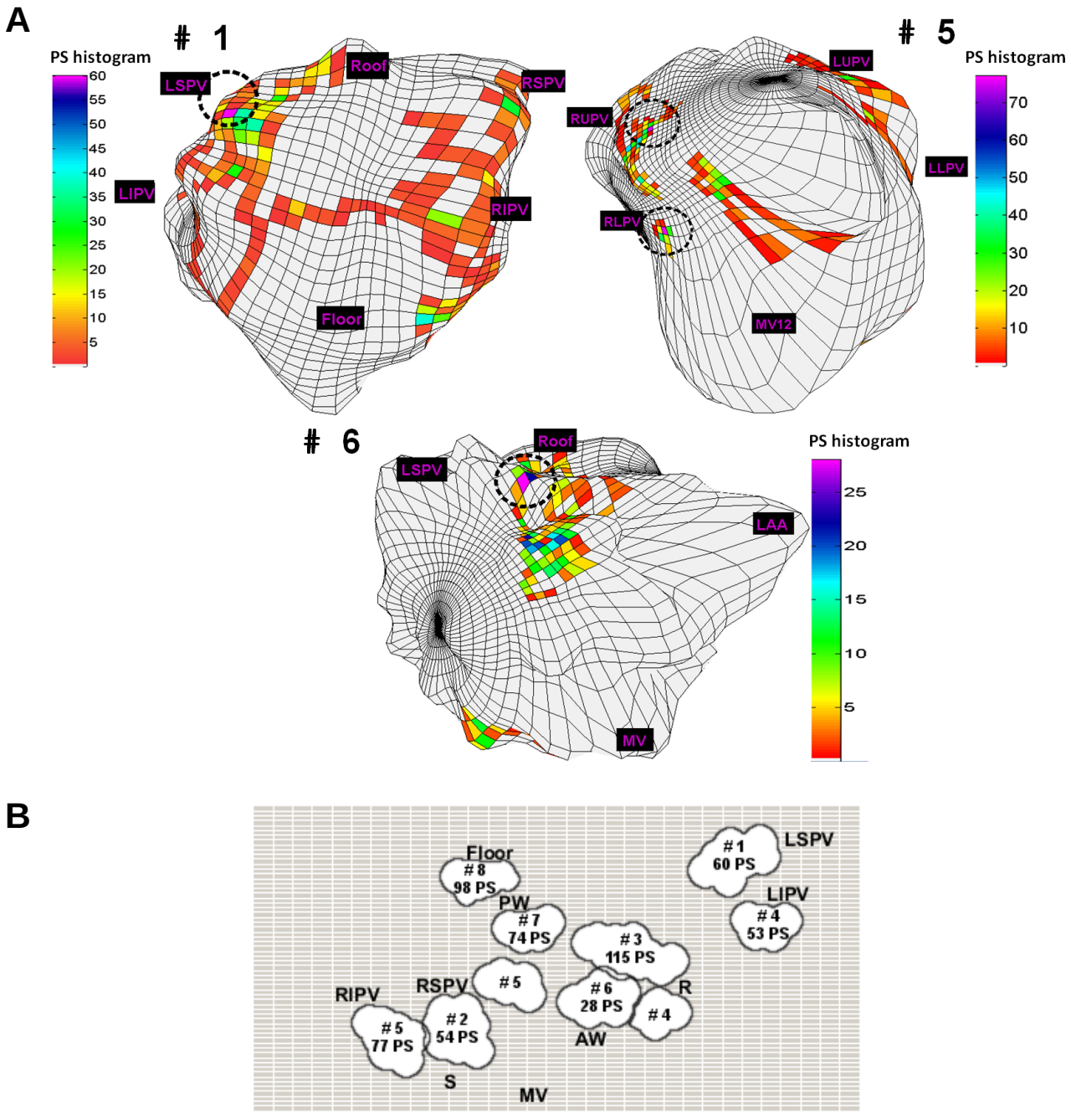


Figure 3 - A sample case of PS histograms demonstrating the presence of preferential PS areas. The 3D maps were obtained by calculating the incidence of PS points over 15 s segments. (A) 3D view highlighting the PS histogram of three distinct patients. In both cases, areas near the PVs are observed with higher PSs incidences; (B) a 2D view

summarizing the observed clusters but now extended to all patients in baseline. (RSPV: right superior PV; RIPV: right inferior PV; LSPV: left superior PV; LIPV: left inferior PV; R: roof; PW: posterior wall; AW: anterior wall; MV: mitral valve; S: septum).

# Figure 4

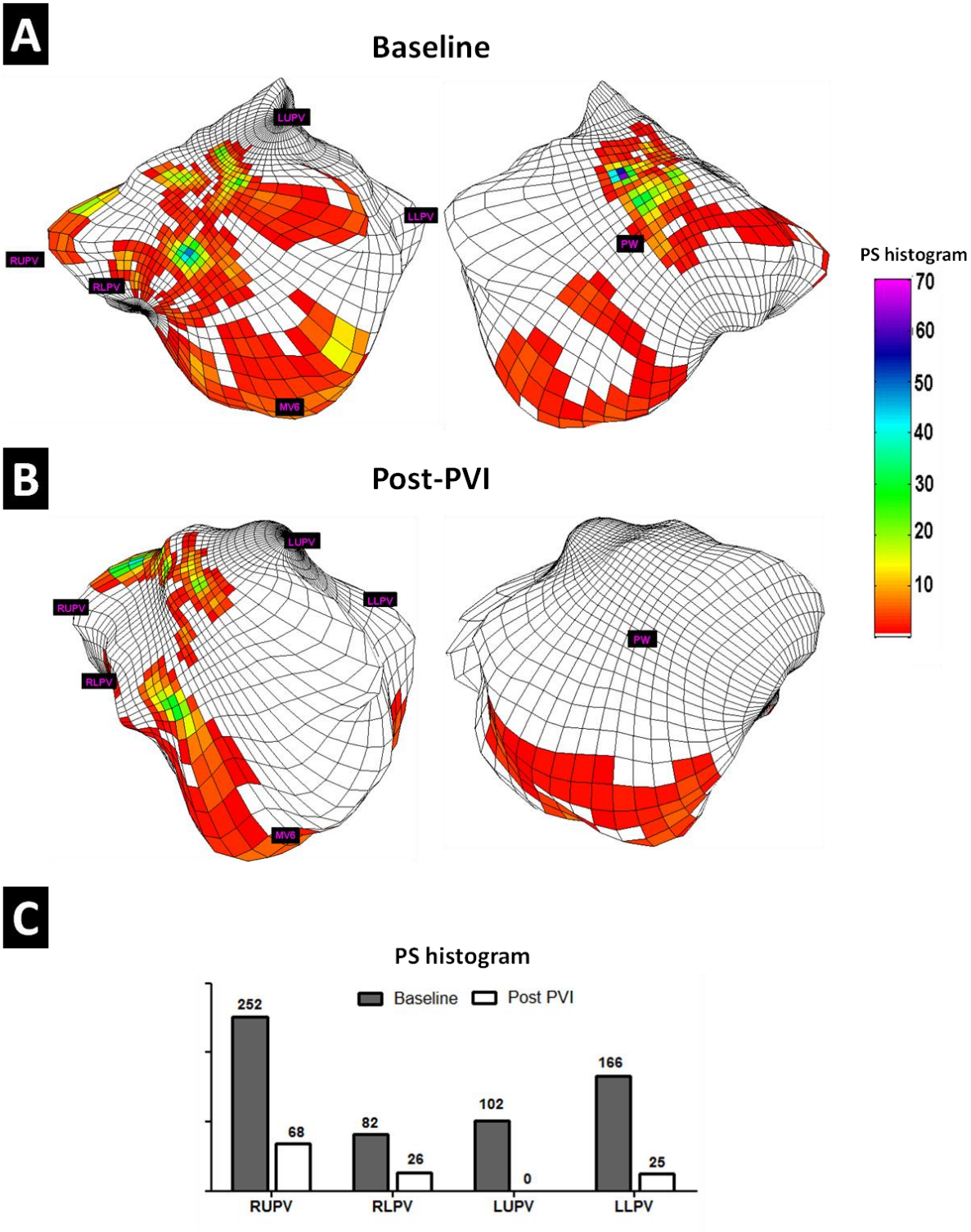
A
Baseline
LUPV
LLPV
RUPV
RLPV
MV6
PW
PS histogram
70
60
50
40
30
20
10
B
Post-PVI
LUPV
LLPV
RUPV
RLPV
MV6
PW
C
PS histogram
Baseline
Post PVI
252
68
82
26
102
0
166
25
RUPV
RLPV
LUPV
LLPV

Figure 4 - Impact of substrate modification on PS incidence after PVI ablation. A 3D view of a color-coded PS incidence map highlighting the frequency of PSs occurrences identified in a 15 s period in a sample patient for baseline (A) and post-ablation (B) highlighting a general reduction of the areas, number of occurrences and complexity of the PSs post PVI. In (C) summary of the overall PS incidence for all patients in the PVs area before and after PVI.

564

# Figure 5

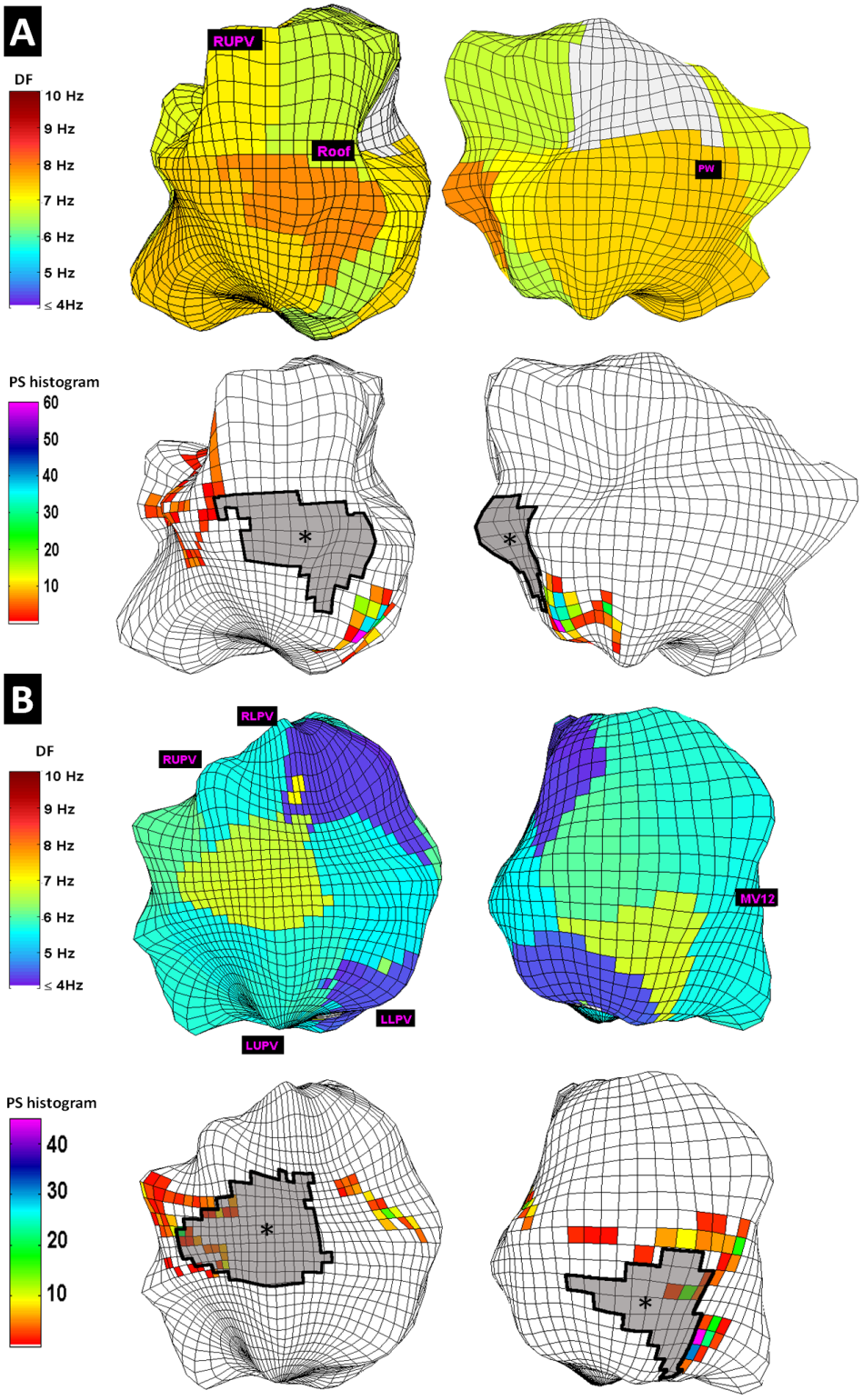


565

Figure 5 - Spatiotemporal correlation between HDF areas and highest PS incidence. A pattern where the PS points were concentrated surrounding the HDF areas is presented (A); and the PS points were present either on areas surrounding HDF or just inside the boundaries of the HDF areas (B).

# Figure 6

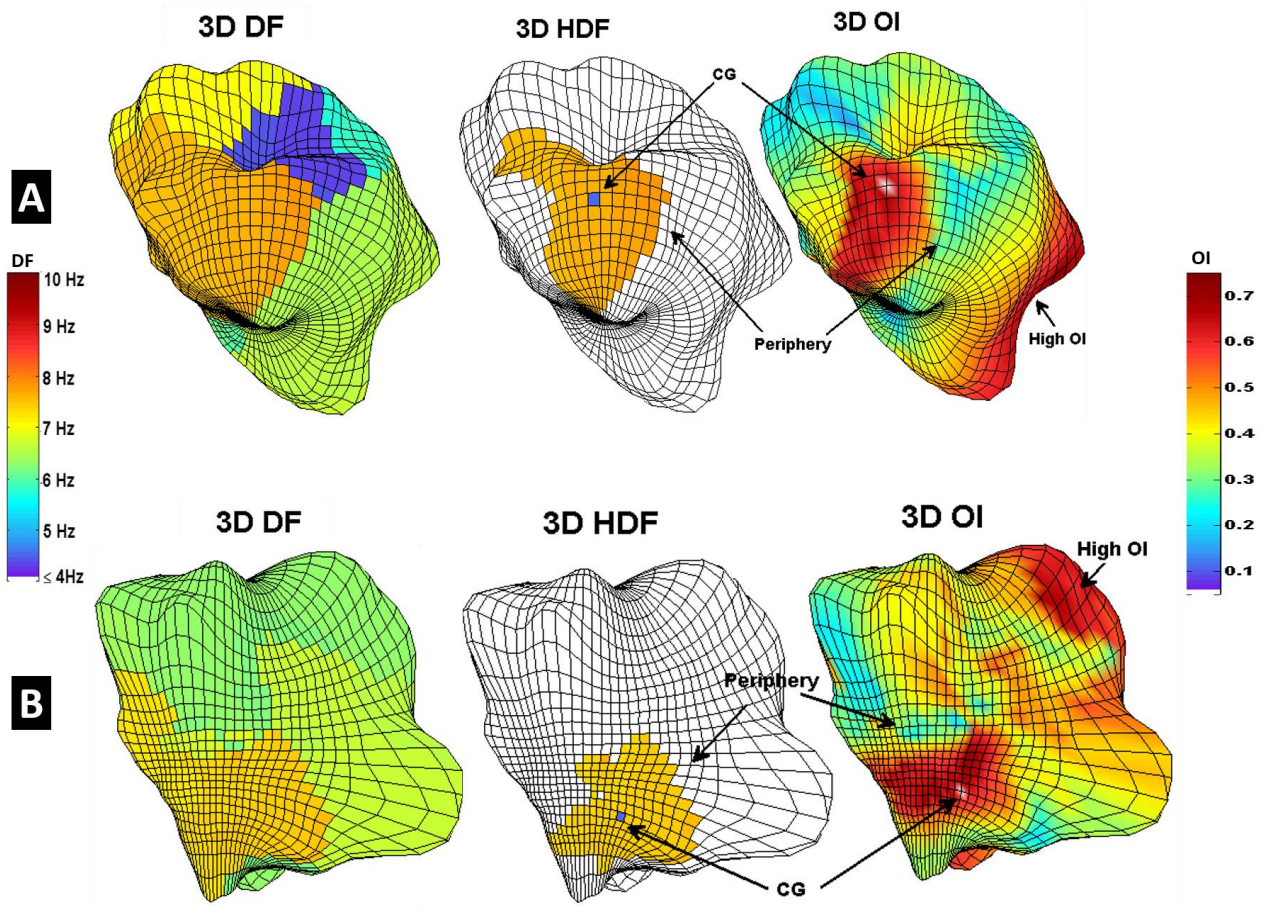


Figure 6 - Illustration of two sample cases of DF and OI mapping focusing on the HDFA identification (A and B). 3D representation including the mapping of the DFs (Left) and its respective HDFA (Middle). DF organization from the HDFA shows that the OI at the core has a higher organization when compared with its periphery and increases again in some remaining LA areas (Right).